Regulation of the Phage Lambda Viral Packaging Motor's Grip and DNA End-clamp Mechanism

Brandon Rawson[1], Qin Yang[2], Carlos E. Catalano[2], Douglas E. Smith[1]

[1] Department of Physics, University of California, San Diego, La Jolla CA 92093
[2] Department of Pharmaceutical Sciences, Skaggs School of Pharmacy and Pharmaceutical Sciences, University of Colorado Denver, Anschutz Medical Campus, Aurora, CO 80045

Email contacts: des@ucsd.edu, CARLOS.CATALANO@cuanschutz.edu

ABSTRACT

Many viruses utilize ATP-powered motors to package DNA into viral capsids. Here we use single DNA manipulation with optical tweezers and rapid solution exchange to interrogate the dynamics of DNA gripping by the phage lambda motor. Binding of poorly hydrolyzed ATP analogs results in persistent gripping and when slips occasionally occur, the release velocity is very slow, indicating significant friction between the motor and DNA. ADP induces more frequent transitions between gripping and faster slipping. Independent of nucleotides, an "end clamp" mechanism arrests slipping when the end of the DNA is about to exit the capsid. These features are qualitatively similar to those exhibited by the phage T4 motor, although there are some notable differences. Specifically, there are quantitative differences in the DNA grip/release kinetics and their dependence on nucleotides and applied force. But the most striking difference is that there are frequent long pauses during DNA exit from the capsid even in the absence of nucleotides. This pausing occurs at low capsid filling and does not increase with length of DNA packaged, indicating that it is not caused by jamming/knotting of the packaged DNA, but is attributable to fluctuation of apo-state motor subunits into a DNA gripping conformation. This finding supports our previous hypothesis that pauses which are frequently observed during packaging are caused by fluctuation of motor subunits into such conformation. Overall, compared with T4, the lambda motor exhibits stronger interactions with DNA, which may be attributable to the small terminase subunit in the lambda packaging motor complex.

INTRODUCTION

Many dsDNA viruses employ an ATP-powered molecular motor during assembly to package their genomes into viral procapsid shells[1,2,3,4]. The motor translocates the DNA into the capsid through a portal nanochannel. Many bacterial viruses (phages), and some human viruses such as herpesviruses, follow this mode of assembly. The motor exerts large forces to pack the DNA to densities as high as ~0.65 g/ml, overcoming resistive forces arising from factors including electrostatic self-repulsion of negatively charged DNA segments, DNA bending rigidity, and entropy loss[5,6,7,8,9,10]. Besides playing a critical role in virus assembly, packaging motors are also models for investigating general biomotor principles as they have homologies with many cellular motors, including helicases, chromosome transporters, and protein translocases[11,12,13].

In previous work, we developed methods using optical tweezers to measure the packaging of single DNA molecules into single viral capsids, applied to phages phi29, T4, and lambda[14,15,16,17,18]. These motors were found to generate remarkably high forces (>60 pN) and translocate DNA at speeds as high as ~200-2000 bp/s. The optical tweezers method, combined with site-directed mutagenesis of motor proteins and modified DNA substrates, has been extensively applied to interrogate detailed motor mechanisms[19,20,21,22,23,24,25,26]. Complexities in the functions of these motors include: (i) velocity fluctuations and pauses and slips that occur during DNA translocation, (ii) a coordinated "burst-dwell" mode of incremental translocation steps by multiple motor subunits, (iii) variable DNA rotation and step size during duplex translocation, and (iv) allosteric regulation of translocation velocity[27,28,29,30].

We recently developed a method to probe the motor's DNA gripping mechanism, first applied to phage T4[31]. Packaging is initiated in a solution containing ATP and then the ATP is suddenly removed, and various nucleotides then added (or removed) by rapid solution exchange. In the absence of nucleotides, we found that the T4 motor releases its grip and the DNA slips out at speeds of ~1,500-2,500 bp/s with only a small ~3 pN resisting friction force. In contrast, addition of a saturating concentration of poorly hydrolyzed ATP analog induces the motor to grip the DNA most of the time. This showed directly that ATP binding induces motor subunits to undergo a conformational change that causes them to tightly grip DNA. An unexpected finding was that when occasional slipping occurs with ATP analog bound, the transient slipping velocity is much slower than with no nucleotides, indicating that nucleotide binding also increases the friction between the DNA and non-gripping motor subunits. The hydrolysis product, ADP, was found to induce frequent transitions between gripping and slipping with variable velocities, suggesting it induces variable motor conformations.

Structural studies of several phages indicate that the motor consists of a ring of five subunits surrounding the DNA[32,33,34]. Initial models proposed that subunits grip the DNA one-at-a-time[20,32,28,29,31]. However, recent structural studies of phage phi29 showed that the motor can have either a planar ring or helical split-ring conformation[35]. These studies, combined with biophysical studies[36], led to a proposed model in which, in the helical conformation with ATP bound, all five subunits grip the DNA simultaneously[37]. The subunits then sequentially hydrolyze ATP and undergo conformational changes that bring the ring step-by-step back towards a planar conformation. This model, which proposes that multiple subunits interact with the DNA simultaneously, seems to fit with the evidence from our T4 studies that multiple ATP-analog-bound subunits interact strongly with the DNA during slipping[31].

Here, we apply the optical tweezers method to study the DNA grip/release dynamics of the phage lambda motor to investigate if the behavior observed with phage T4 is universal. The packaging

function of the lambda motor has previously been extensively investigated via genetic, biochemical, and single-molecule studies[38,17,39,40,22,23,41,42,24,25,26]. Our previous finding that decreasing ATP concentration causes increased back slipping of the DNA during packaging provided evidence that ATP binding to the motor induces DNA gripping. Site-directed mutagenesis studies also showed that changing certain residues in the motor's ATP binding site causes increased slipping[24,25]. We have also used gel electrophoresis to analyze the retention of DNA in lambda complexes packaged in bulk in vitro reactions and found that ATP hydrolysis is required to retain the genome at the end of packaging[43]. GTP, ADP, and the poorly hydrolyzed ATP analog AMP-PNP were also found to stabilize the packaged genome. The ATP analog γ-S-ATP was found to provide only partial stabilization, but we found that it can be used to temporarily stall partly packaged complexes, and these can then be restarted in the optical tweezers assay by moving them into a solution containing ATP[18]. However, the electrophoresis studies observed that the fully packaged genome slowly leaks out of capsids on the timescale of hours[43].

The present studies probe DNA release by a stalled lambda motor and characterize the detailed DNA grip/release dynamics in real time and dependence on nucleotides. In these studies the lambda motor complexes are assembled with both the large terminase protein, containing the ATPase that powers DNA translocation, and small terminase subunit, implicated in initiation of packaging[38,39]. We confirm here, like our findings with phage T4, that ATP-analog binding induces persistent DNA gripping and that when occasional slipping occurs it is much slower than slipping in the absence of nucleotides[31]. We similarly find that ADP induces frequent transitions between gripping and slipping and that lambda also has an "end clamp" mechanism that prevents the whole DNA from slipping out[31]. However, we observe quantitative differences in the grip-slip dynamics between lambda and T4, and a striking qualitative difference is that the lambda motor frequently grips DNA even in the absence of nucleotides.

RESULTS

DNA gripping/slipping measurement

We first initiate DNA packaging in a bulk reaction with empty lambda procapsids, recombinant terminase proteins from an extract from *E. coli*, and ATP, using protocols described previously[18,24]. In brief, after a short incubation for 45 s, we add the poorly hydrolyzed ATP analog γ-S-ATP to stall the reaction. These complexes are tethered to microspheres and manipulated with optical tweezers as illustrated in Fig. 1. The capsid is attached to one microsphere and the end of the DNA hanging out is attached to a second microsphere. The complex is then brought near a microcapillary tube dispensing a solution containing ATP to restart DNA packaging, and a small force is applied to stretch the DNA so that its length can be accurately measured. After 1.5-6 kbp of DNA is packaged (a small fraction of the 48.5 kbp lambda genome length), the complex is rapidly moved out of ATP into a solution containing either no nucleotides or a saturating concentration (0.5 mM)[44,45] of poorly hydrolyzed ATP analogs (γ-S-ATP or AMP-PNP) or ADP (Fig. 1). The measurements were conducted at room temperature (23 °C). No further packaging is detected after the solution exchange, indicating that, with ATP analogs, even if some hydrolysis is occurring it is either very slow or not facilitating DNA translocation. The DNA is thus either being gripped by the motor or slipping out of the capsid. We repeated these measurements on an ensemble of individual complexes for each condition.

Examples of individual measurements of the length of DNA that has exited the capsid versus time are shown in Fig. 2A. In all four solution conditions we observe dynamic transitions between DNA

gripping and slipping, but the presence of nucleotides causes significant differences (Table 1). With no nucleotides, the DNA mostly slips out of the capsid (56% of the time). In contrast, when a saturating (0.5 mM) concentration of γ-S-ATP or AMP-PNP is added the DNA is almost always gripped (97-99.6% of the time). This shows that ATP-analog binding induces motor subunits to undergo a conformational change that allows them to persistently grip the DNA. When the same concentration of the hydrolysis product, ADP, is added the DNA is also frequently gripped (~83% of the time), but this is notably less persistent than with the ATP analogs. With the ATP analogs, since slipping is very infrequent, the average DNA exit velocity (including the pauses due to gripping events) is extremely slow (0.5-1.7 bp/s). The average exit velocity is higher with ADP (11 bp/s) and highest with no nucleotides (59 bp/s).

While nucleotide binding induces more persistent gripping, in qualitative accord with our findings with phage T4, a striking difference is that the lambda motor frequently grips the DNA in the absence of nucleotides. With T4, there are almost no pauses during slipping[31], whereas for lambda there are pauses ~44% of the time (see Fig. 2B). Due to these pauses the average DNA exit velocity is 34x slower than that measured for T4.

To further characterize the dynamics, we calculated the transient velocities during slipping in a 1 second sliding time window, using the same analysis protocols as in our previous T4 studies (Table 1 and Fig. 3). With no nucleotides, the transient velocity is usually between 0 and ~350 bp/s, with ADP usually 0 to ~250 bp/s, and with γ -S-ATP or AMP-PNP usually <100 bp/s. Thus, not only is DNA gripping different in the different motor nucleotide binding states, but the transient velocities during slipping are different. This indicates that nucleotide binding not only regulates DNA gripping, but also affects the strength of interactions between the motor subunits and DNA even when the duplex is not gripped.

Motor gripping with no nucleotides

The frequent pauses observed during slipping with no nucleotides, when all motor subunits are in the "apo" state, is surprising as this was not seen with phage T4. We analyzed these pauses to determine their frequency and durations (Table 1). We considered the possibility that these pauses could be caused by jammed or knotted conformations of the DNA that impede its exit, but this seems unlikely as it was not observed at equivalently low capsid filling levels in phages T4 or phi29[31,46]. Also, computer simulations of viral DNA ejection do not predict that knots would cause pauses[47], and the likelihood of DNA jamming or knotting is expected to increase with increasing packaged DNA length[48,49,50]. In fact, we find that the frequency of pauses *decreases* with increasing length of DNA packaged (Fig. 4). We therefore attribute the pauses to transient DNA gripping by the motor despite the absence of nucleotides. The average pause duration (2.07 s) thus corresponds to the average lifetime of a gripping event and the average slip duration (1.95 s) to the average time it takes the motor to re-grip the DNA.

Another notable feature is that the transient slipping velocities are much lower than observed with T4 (Fig. 3 and Table 1). The average slipping velocity is 133 bp/s with 5 pN applied force, which is ~15-fold lower than measured for T4, but still much faster than that exhibited by lambda with poorly hydrolyzed ATP analogs (~40-46 bp/s). This slipping is measured with 5 pN applied force and <20% of the genome length packaged, when there is negligible force resisting DNA confinement[17,51]. Therefore, we infer that there is an opposing 5 pN friction force on the DNA when slipping occurs at this speed[31]. This is attributable to intermolecular interactions between the DNA and the motor and portal channels, and

potentially also the inner walls of the capsid, and to hydrodynamic drag. We observe wide variation in the transient slipping velocities (Fig. 3), which indicates that this friction fluctuates, presumably due to fluctuations in the conformation of the motor and/or portal rings.

Motor gripping with poor hydrolyzed ATP analogs

Addition of the saturating concentration (0.5 mM) of γ-S-ATP or AMP-PNP results in almost continuous DNA gripping (Table 1). With γ-S-ATP the DNA is gripped 97% of the time, which is notably higher than the 84% measured for T4 in the same conditions. This difference may be attributable, in part, to the frequent gripping by the lambda motor even in the absence of ATP. With AMP-PNP, which was not tested in the T4 studies, we find that the DNA is gripped an even higher fraction of time (99.6%). Thus, binding of ATP analogs locks the motor in a nearly static grip. The slightly lower gripping fraction measured with γ-S-ATP, when compared to AMP-PNP, is likely attributable to a higher dissociation and/or hydrolysis rate for this analog since ATP or ADP dissociation increases the chance of motor grip release. In total, these findings are generally consistent with prior models for motor function that predict that ATP binding induces DNA gripping and predict that motor subunits release their grip after hydrolysis and product release[4,20,28,32,24,37].

When slipping does occasionally occur, the average transient slipping velocity (~40-46 bp/s) is much lower than that measured with no nucleotides (Table 1). This indicates that motor subunits in the ATP-bound state, even when they are not gripping the DNA, are in a conformation that exerts higher friction that slows the slipping. In this state the average velocity is close to that measured for T4 (~34 bp/s)[31]. This suggests that both motors may have a similar conformation and interaction with the DNA in the ATP-bound state, and that the main difference is that lambda motor has a higher tendency to fluctuate into higher friction or gripping conformation in the apo and ADP-bound states. The slipping here is again occurring against the 5 pN applied force and indicates that there is 5 pN resisting friction force at this slipping velocity. The friction is "higher" than it is in the apo state in the sense that intermolecular and hydrodynamic friction forces are expected to be a monotonically increasing function of velocity[52]. When there is slower slipping in one condition with the same applied force as in a different condition, this indicates there is a stronger influence of friction (or higher effective friction coefficient) in the former case.

The difference in average slipping velocity occurring with γ-S-ATP versus without nucleotides isn't as striking as it is with T4, displaying just a 2-fold reduction versus a ~60-fold reduction for T4. The maximum slipping velocity exhibits only a ~4-fold reduction (from 670 to 158 bp/s). These findings are consistent with the notion that lambda motor subunits in the apo state are more likely to spontaneously fluctuate into either a gripping conformation or one that exerts high friction.

Motor gripping with ADP

During DNA translocation each motor subunit has a state where, after binding ATP and hydrolyzing it, the binding pocket is transiently occupied by an ADP molecule. We find, with the saturating concentration (0.5 mM) of added ADP, that the DNA is gripped 83% of the time (Table 1). This is more persistent than in the absence of nucleotides (44%) but less than with the poorly hydrolyzed ATP analogs (97-99.6%). Analysis of the individual gripping events indicates that their frequency is ~4x greater than with no nucleotides, and their average duration is ~2.3x greater. This demonstrates that the binding of ADP to motor subunits causes gripping, but this state is less stable than when the ATP

analogs are bound. These results are qualitatively in accord with our findings with phage T4 and consistent with the model that one of the causes of the slips is dissociation of ADP from gripping motor subunits[31]. That there is a ~2.3-fold reduction in slip duration with ADP, when compared to no nucleotides, suggests that slipping can be arrested by re-binding of ADP. The situation is more complex than for T4, however, since there are significant transitions between gripping and slipping even in the absence of nucleotides. A striking quantitative difference is that the lambda motor grips a ~18-fold higher fraction of the time than the T4 motor in the same condition.

Binding of ADP also causes a reduction in transient slipping speed. The average slipping speed is 77 bp/s with ADP compared to 40 bp/s with AMP-PNP and 120 bp/s with no nucleotides. This demonstrates that, like the situation with bound ATP analogs, motor subunits in the ADP-bound state not only grip the DNA more frequently than in the absence of nucleotides, but they also exert higher friction on the DNA. Since this slipping speed is measured with 5 pN applied force, this again implies that the resisting friction force is 5 pN. A notable difference here is that the slipping speed is ~12x slower on average than that measured for T4. This contrasts with the situation with the ATP analogs where the slipping speeds are similar. This indicates that with ADP bound there is must stronger friction between the motor and DNA with the lambda motor. This is likely attributable, in part, to the much more significant friction acting even in the apo state. There is also variation in the slipping velocity in this condition (Fig. 3), which again indicates that the friction is variable, but it is notably much less variable than observed for T4. The range of the slipping velocities with ADP is entirely within the range measured with no nucleotides, whereas with T4 the slipping is almost always slower with ADP[31]. This indicates that motor-DNA friction with ADP bound is less variable than with the T4 motor.

Dependence of motor gripping on applied force

The measurements described above were with 5 pN applied force. Although this is small compared with the maximum force the motor can exert during DNA packaging (>50 pN)[17], we would still expect to see a dependence of the gripping/slipping on applied force. First, the slipping is driven by the applied force with a resulting slipping velocity that depends on the nature of the opposing friction force, which is expected to be velocity dependent[52]. Consistent with this, we find that the transient slipping velocity increases with increasing applied force (Fig. 5A).

The increasing velocity trend is observed both with no nucleotides and with ADP (Fig. 5A). A notable feature is that the velocity is not simply directly proportional to force. When the force is increased from 2 to 5 pN (a 2.5-fold increase) the velocity increases by only 1.3x, and when it is increased from 5 to 10 pN (a 2-fold increase) it increases by 1.6x. With ADP, increasing force from 2 to 5 pN increases the velocity by only 1.03x and increasing it from 5 to 10 pN increases it by only 1.3x (Fig. 5A). This weak dependence suggests the dominant source of friction is intermolecular sliding friction, likely between the DNA and portal-motor channel surfaces, and not hydrodynamic friction[52]. The weaker dependence on force observed with ADP is also consistent with the friction being stronger and even more strongly dominated by sliding friction between the DNA and motor.

Second, in both conditions (apo and ADP) we observe that the fraction of time spent slipping increases with increasing force (Fig. 5B). This is consistent with our expectation that increasing force could: (i) lead to accelerated rupture of the motors grip, and (ii) hinder re-gripping (since it would have to occur from a higher slipping velocity). Indeed, from our analyses of the individual gripping and slipping events, we find that the average duration of gripping events decreases (Fig. 6A) and their

frequency decreases with increasing force (Fig. 6B). It is also notable that, in the absence of nucleotides, increasing force from 2 to 10 pN has a stronger influence on gripping frequency (decreasing it by 3.4x) than on average grip duration (decreasing it by 2x), whereas with ADP both gripping frequency and average grip duration are reduced 2.1x. This is consistent with hindered re-gripping having a stronger effect when motor subunits are in the apo state, and the slipping is faster. The finding that the average duration of slips increases more strongly with increasing force for the apo condition than with ADP (Fig. 6A) supports this conclusion.

DNA End Clamp Mechanism

In the absence of nucleotides there is slipping 54% of the time, such that the DNA exits the capsid at an average rate of 120 bp/s. At this rate, the full lambda genome would exit the capsid in ~7 minutes, so the complex would not be very stable if ATP were lost during packaging (e.g., due to environmental fluctuations). Restarting packaging would require re-association of components which, depending on their concentrations, may be slow/inefficient. In our studies with phage T4 we discovered a remarkable DNA "end clamp" mechanism that mitigates this problem[31]. Here we show that phage lambda exhibits the same mechanism.

Independent of the length of DNA initially packaged, slipping suddenly arrests when the end of the packaged DNA is about to slip out of the capsid (Fig. 7A). This occurs when the measured length of the DNA outside the capsid is roughly 10 kbp, which is consistent with the packageable length of the DNA substrate (~10 kbp). This behavior was repeatable in every individual measurement except in a few cases where the tether detached before the whole DNA slipped out (attributable to detachment of the capsid from the microsphere). The clamping also occurs in all the solution conditions studied (with γ-S-ATP, AMP-PNP, ADP, and no nucleotides), which shows that it is independent of the nucleotide binding states of motor subunits.

The end-clamped complex is stable on the timescale of at least several minutes even with a 10 pN force applied. Like with phage T4, after the DNA has been end-clamped we find that packaging can be reliably restarted by moving the complex back into the solution containing ATP. We also find that packaging, slipping, end clamping, and re-packaging can be repeated multiple times with individual complexes. No obvious differences in the packaging or slipping/gripping dynamics were observed in repeated measurements with a single complex (Fig. 7B).

The measured ~1-2 kbp variations in the final length of the DNA released after slipping arrests (Fig. 7) are attributable to limits of the accuracy of the absolute length measurement. However, the multiple slip/clamp/re-package events allow us to precisely check the repeatability of the end clamp position. The measured length differences following repeated clamping events has a standard deviation of only 32 bp (Fig. 7C), which indicates that the DNA is being clamped exactly at, or very near to its end. Thus, the end clamp exhibited in the lambda system is functionally identical to that observed with phage T4 and is a robust and stable mechanism that prevents premature loss of previously packaged DNA.

DISCUSSION

We have shown that there are many similarities in the grip/slip dynamics exhibited by the viral packaging motors of the lambda and T4 phages. In both systems, the binding of poorly hydrolyzed ATP analogs induces highly persistent gripping of the DNA substrate. These results are consistent with our

previous observation that when the concentration of ATP is reduced during lambda packaging this causes increased slipping[24], and shows that ATP binding induces tight DNA gripping whereas nucleotide dissociation promotes release of the grip. We also find in both systems that ADP binding induces DNA gripping, but this is less persistent than with the ATP analogs. This is consistent with the need for motor subunits, during translocation, to be capable of holding the DNA until the end of each hydrolysis event, but then being able to release it so the motor can grip and translocate the next section of DNA. These features are generally in accord with the models for lambda packaging motor function described in several of our recent publications[24,26,4], but illustrate new features not included in the previous models.

Another feature exhibited in both systems is that ATP analog or ADP binding increases the strength of motor-DNA interactions even during periods when the motor is not tightly gripping the DNA. The slipping velocity is much lower than in the absence of nucleotides and indicates that nucleotide binding causes motor subunits to be in a conformation where they exert higher friction on DNA on average. This effect may serve a useful purpose to limit the extent of DNA back slipping which we have previously observed to occur during DNA packaging[17,24]. The similarity in the features described here for lambda and T4 support the notion that there is a high degree of universality in the mechanisms of viral motors.

The present results are harmonious with our previous studies which used gel electrophoresis to analyze the retention of DNA in lambda complexes packaged in bulk in vitro reactions[43]. It was found that after packaging the full 48.5 kbp lambda genome, using 0.2 mM ATP, that addition of an excess (2 mM) of AMP-PNP or ADP resulted in a highly stable complex in which the DNA was mostly retained after 1-4 hrs. The finding with AMP-PNP is consistent with our present finding of an average DNA exit rate, with AMP-PNP of only 0.47 bp/s, which we showed is due to a combination of frequent gripping of the DNA by the motor and very slow slipping due to motor-DNA friction. At this rate only 1.7-6.8 kbp would exit after 1-4 hrs., which is a small fraction of the 48.5 kbp genome length so the change would likely not be resolved by electrophoresis.

We note that three factors could also cause the DNA exit to be slower in the bulk packaging study compared with the present findings. First, for the case where the full genome is packaged, the initial DNA exit would be additionally slowed due to the high DNA packing density, which results in a reduced molecular mobility[53,46]. Second, in the single-molecule measurements we are applying a 5 pN force which causes increased exit velocity and decreased % time gripping (Fig. 5A&B). Third, the bulk reaction had 0.2 mM ATP during packaging, which alone was found to cause ~50% of the packaged DNA to be retained after 1-4 hrs, so this could further slow the exit. Since the complexes in the single-molecule assay are immobilized on trapped microspheres we have complete solution exchange and thereby remove all residual ATP. In this case the DNA exits at 59 bp/s on average.

The finding in the bulk assays that addition of ADP also resulted in retention of most of the DNA after 1-4 hrs is also consistent with our finding of an average DNA exit rate of 11 bp/s. If exit of the full genome occurred at this rate, it would take ~1.2 hrs, on average. The factors discussed above that would make DNA exit in the bulk experiments slower would apply here as well. The bulk assays also found that addition of γ-S-ATP after packaging results in loss of >90% of the packaged full-length DNA after 1-4 hrs, but in this case the gel electrophoresis showed that shorter fragments typically around ~30 kbp remained packaged, suggesting that ~20 kbp typically exits. This would correspond to an exit rate of 1.4 bp/s, which is consistent with the average exit rate of 1.7 bp/s we measure in the single-molecule assay with γ-S-ATP, again considering the factors that would make the bulk experiments slower. As with the

AMP-PMP, our present studies show that the slow exit with this ATP analog is due to a combination of gripping and slowed slipping.

Both lambda and T4 exhibit the DNA end clamp mechanism that prevents the entire length of DNA from slipping out of the capsid even in the absence of nucleotides. As we pointed out previously[31] this mechanism would increase the efficiency of packaging since it ensures that the initiation of DNA translocation is essentially irreversible. For example, if motor slipping occurred when only a small length of DNA was packaged, the whole DNA substrate could dissociate from the complex without the end clamp. When packaging occurs inside infected host cells increasing the efficiency of packaging and minimizing the time required is advantageous to the virus because the viral DNA is subject to degradation by exonucleases[54].

How the end clamp works remains unclear. One possibility is that the motor can detect the amount of DNA remaining inside the capsid (e.g., via an allosteric signal) and is triggered to clamp the duplex when the capsid is nearly empty. In fact, such a mechanism could explain our surprising observation in Fig. 4 that the frequency of DNA gripping by the motor in the apo state increases with decreasing length of DNA remaining in the capsid. Another possibility is that the motor (and/or portal ring) specifically recognizes the end of the DNA as it is slipping out through the channel and clamps it. A third possibility is that the end of the DNA is simply anchored some place inside the capsid.

While the behavior of the lambda motor exhibits many similarities with T4, as summarized above, we do find some significant differences. Overall, the lambda motor exhibits significantly stronger interactions with the DNA substrate. With ADP, gripping is significantly more frequent and slipping velocity slower. With γ-S-ATP, the gripping is highly persistent in both systems, but is again notably higher for lambda (97% vs. 84%-time gripping).

Most striking is the occurrence of frequent DNA gripping by the motor even in the absence of nucleotides and highly slowed velocity during slipping, which was not observed with T4. In previous work we observed that there is also frequent pausing during DNA packaging by the lambda motor with saturating ATP. The cause of these pauses was unknown but we hypothesized that they could be attributable to the motor spontaneously fluctuating into a conformation where it can grip DNA despite not binding ATP. Our present results directly confirm that this can occur and thus provide strong support for this hypothesis. Notably, the measured average duration of the pauses in packaging (2 s) is approximately equal to the average duration of the gripping events we detect here in the absence of ATP (2.1 s).

A possible explanation for some of the differences exhibited by lambda compared with T4 could be that the lambda motor complex in the present study was assembled with both the large terminase subunits (TerL), which harbor the ATPase responsible for driving translocation, and the small terminase subunits (TerS), which play a role in the initiation of packaging[24,38,39]. In contrast, our prior measurements with T4 used motor complexes assembled only with TerL[31]. TerS is an integral component for packaging in vivo, but it is unknown whether it has any effect on DNA gripping or translocation dynamics. However, it is possible that its presence could explain the stronger motor-DNA interactions observed here with lambda. A potential approach to investigate this in future studies would be to try find conditions where lambda could be measured without TerS and/or conditions where T4 packaging could be measured with TerS.

The kinetic model we proposed previously to describe the observed slipping/gripping dynamics with T4[31] can be modified to account, at least qualitatively, for the different behavior observed here. First, a pathway that allows fluctuation of motor subunits in the apo state into a conformation that can alternately grip or exert high friction on the DNA would need to be added. Second, the "minimum friction" motor conformation proposed to explain the very high velocity slipping observed in the apo state, and sometimes in the ADP bound state, would need to be eliminated. This model is, however, based on the assumption introduced in previous models[20,27,28,32], that only one subunit grips the DNA at a time. Recent studies of phage phi29 led to a proposed model in which multiple ATP-bound subunits grip the DNA simultaneously[35,37]. If this behavior were found to apply to lambda and T4, it would require the kinetic model proposed earlier to be revised. In particular, dissociation of nucleotide from one subunit might not be sufficient to explain the onset of slipping events (although it is possible that not all subunits may grip the DNA with equal strength). The model could be revised to describe slipping as primarily occurring due to force-accelerated rupture of the motor's grip while one or more subunits are in a conformation where they have the capacity to grip DNA. The slow slipping observed with ATP analogs could then be explained, in the simplest scenario, as being due to subunits in this same conformation exerting high friction on the DNA. Arrest of slipping could then occur spontaneously while the subunits remain in this conformation.

MATERIALS AND METHODS

Phage lambda procapsids

Lambda procapsids were obtained from *E. coli* lambda lysogen NS428, provided by Michael Feiss and Jean Sippy (University of Iowa), as described previously[24]. The strain contains a mutated gene preventing packaging, resulting in an accumulation of empty procapsids. The lysogen was grown to OD600 of 0.3 at 32 °C before being induced by moving to 45 °C for 15 minutes and then 38 °C for 60 minutes. After induction the culture is pelleted and resuspended in 0.5 ml TMS (50 mM Tris, pH 7.8, 10mM $MgCl_2$, 100 mM NaCl) containing 40 units RNase-free DNase (Roche). The lysate was clarified by centrifuging at 10,000 rpm for 10 minutes, followed by 13,000xg for 3 minutes. The supernatant was then loaded on top of a linear 10-30% sucrose gradient in 0.5x TMS buffer (25 mM Tris, pH 7.8, 5 mM $MgCl_2$, 50 mM NaCl) and centrifuged at 40,000 rpm for 64 minutes. The band that contains the procapsids was collected and detected by observing the scattering of a light beam off the procapsids. They were then diluted in TMS buffer and pelleted at 40,000 rpm for 102 minutes. The pellets were re-suspended in a total of 200 µl TMS buffer by standing at 4 °C overnight. They were then re-banded on a second set of sucrose gradients, pelleted, and resuspended in a final volume of 100 µl and stored at 4 °C.

Terminase proteins

Terminase proteins were obtained from *E. coli* extracts, as described previously. In brief, the *E. coli* lysogen OR1265 was grown at 32 °C for 8 hours in a 5 mL culture of TB broth and 50ug/ml Amp before being transferred to a 50 mL TB-Amp broth to grow overnight. The overnight culture is then used in its entirety to inoculate a 1 L TB-Amp and grown to an OD600 of 0.6 before being induced by adding 1L of 62 °C TB broth. The induced cells are then grown at 45°C for 15 minutes, followed by 45 minutes at 42°C. The cells are then pelleted by centrifuging at 5000 g for 20 min before being stored at -80°C. The pellet is then resuspended in 50 mL of low imidazole His Buffer (20 mM Tris pH 8.6, 500 mM NaCl, 10% glycerol, 7 mM β-Me, 20 mM imidazole), 500 µl GE's PI, and lysozyme at 0.4 mg/ml and kept on ice for 30 minutes. The cells are then sonicated using 10 sets of 10 seconds at a 90% duty cycle before finally

centrifuged at 13,000g for 30 min. The supernatant containing the terminase proteins is then removed and stored at either -20°C for short term or -80°C for long term storage.

DNA substrate

A 13,881 bp plasmid, named as pJM1, containing the full λ *cos* site, which is necessary to initiate packaging, was previously prepared by the Feiss Lab (University of Iowa), as described previously[24]. This plasmid is extracted and purified from the relevant *E. coli* strain by use of a Qiagen plasmid miniprep kit. Post purification the plasmid was cut with restriction enzyme NcoI-HF and ran out on a gel to verify the size. Labeled PCR primers were bought from IDT Inc. The sequences of the forward and backward primers were Dig-5'-TCGATAATCGTGAAGAGTCGGCGAGCCTGGTTAG-3' and Biot-5'-TACGTCGAAGTGACCAACTAGGCGGAATCGGTAG-3' respectively. Dual labeled DNA was PCRed was generated by PCR39 using the TaKaRa LA Taq kit (Takara Bio, Inc), resulting in a 13,681 bp biotin-labeled dsDNA for use in packaging. The *cos* site is downstream and results in a ~10.1 kbp substrate for packaging post cleavage.

Single molecule assay

The optical tweezer instrument was calibrated by an established method using DNA molecules as metrology standards[55]. The packaging measurements were done using a slightly modified version of established protocols[18,24]. We use a pre-stalling method in which procapsid-motor-DNA complex is first assembled in a bulk reaction and later restarted. Lambda procapsids, terminase, and pJM1 DNA are mixed in concentrations of 17 nM, 250 nM, and 11 ng, respectively, in a solution consisting of 25 mM Tris-HCl pH 7.5 and 5 mM $MgCl_2$. The mixture is incubated at room temperature for 5 minutes before adding 0.5 mM of ATP. After a shorter 45 second incubation 0.5 mM of γ-S-ATP is added to stall the reaction and prevent the procapsid from packaging the complete substrate.

The procapsid-motor-DNA complex was then mixed with 2.1 µm diameter streptavidin coated microspheres (Spherotech), attaching to the via the biotinylated end of the exposed, prepackaged DNA. This mixture was incubated on a rotating incubator at room temperature for 20 minutes. Lambda antisera, an antibody that binds to the lambda procapsid, was mixed with 2.3 µm diameter protein-G microspheres (Spherotech) at a ratio of 2.5 µl antibody to 5 µl beads (5% w/v) and incubated on the same incubator for 30 minutes. The main flow cell buffer, where grip measurements were conducted, consisted of 25 mM Tris-HCl pH 7.5, 5 mM $MgCl_2$, and 0.05 g L^{-1} BSA. A separate packaging region of the chamber contained the same buffer with the addition of 0.5-1 mM ATP, which was dispensed from a side channel to fuel packaging.

Slipping/gripping analysis

Due to inherent measurement/instrument noise present in every measurement[2] we first conducted a control experiment, tethering just a DNA molecule between two microspheres to calculate the uncertainty in the determination of velocity for a stationary system. For a 1 s detection window this yields an average velocity close to zero (0.004 bp/s), but with a standard deviation (σ) of 14.5 bp/s. This σ characterizes the uncertainty due to Brownian fluctuations and instrument noise. For all the results shown in the figures, except for Table 1, the threshold velocity to identify a period of gripping was set to be 3σ=43.5 bp/s. For the results presented in Table 1 the threshold was set to 2σ to facilitate direct comparison with the previous T4 data which used this threshold[31]. For the results shown in the rest of

the figures here, this threshold was set to 3σ because we found, through analyses comparing the total length slipped with the sum of the lengths of the individual slips, that this provides a more robust method for discerning periods of pausing versus slipping.

Accuracy of the DNA length measurement

The measured variations in the length of the DNA when end clamped (Fig. 7) are attributable to limits of the accuracy of the measurement of absolute DNA lengths with the optical tweezers instrument, primarily due to variations the microsphere sizes, and due to variations in the substrate DNA molecules[31]. The microspheres are nominally 2.1 and 2.3 μm in diameter, but individual microspheres vary by ~300 nm. The length of DNA substrate that can be packaged is nominally 10,052 bp, but due to non-specific priming during PCR there are some molecules with slightly different DNA lengths., which is much smaller than the variability seen in Fig. 7A with measurements of different complexes. The measured length differences following repeated end clamping events have a standard deviation of 32 bp (Fig. 7C). Control experiments in which DNA molecules alone are tethered show that the standard deviation in measured length differences due to instrument noise/drift alone is ~25 bp[31], which accounts for most of the observed variation in Fig. 7C. Thus, the results are consistent with the DNA being clamped exactly at, or very near to its end.

ACKNOWLEDGEMENTS

We thank Mariam Ordyan, Michael Feiss, and Jean Sippy for assisting with preliminary work that demonstrated the feasibility of the studies. This work was supported by NIH grant R01GM118817.

REFERENCES

The references are listed after the figures below.

Table 1. Metrics characterizing the gripping/slipping dynamics, determined from the full ensembles of individual measurements. The T4 results are taken from our Ref. 31. N_m is the total number of individual slipping events measured for each condition. Note that, due to the very low velocity of slipping with the ATP analogs it was not feasible to reliably score individual gripping/slipping events, so frequencies and durations are not reported for those. The periods of slipping were determined using the 2σ velocity threshold criteria (see methods), so that the analysis would match that used in the T4 studies.

	Transient slip velocity (bp/s)	Overall velocity (bp/s)	% Time paused	Grip frequency (#/kbp)	Grip duration (s)	Slip duration (s)	N_m
Lambda (5 pN force)							
Apo	120.2 (10.1)	58.75 (0.4)	44 (2.2)	4.44 (0.37)	2.07 (0.51)	1.95 (0.29)	53
ADP	76.5 (8.5)	11 (0.08)	83 (1.3)	17 (1.5)	4.8 (1.43)	0.86 (0.12)	51
γ-S-ATP	45.8 (3.4)	1.7 (0.03)	97 (1.2)				23
AMP-PNP	39.5 (2.3)	0.47 (0.02)	99.6 (0.13)				23
T4							
Apo	2000 (75)	1960 (75)	2		0.08 (0.02)		25
ADP	885 (90)	844 (93)	4.6		0.28	1.64	35
γ-S-ATP	33.8 (6.3)	2.3 (0.54)	84				9

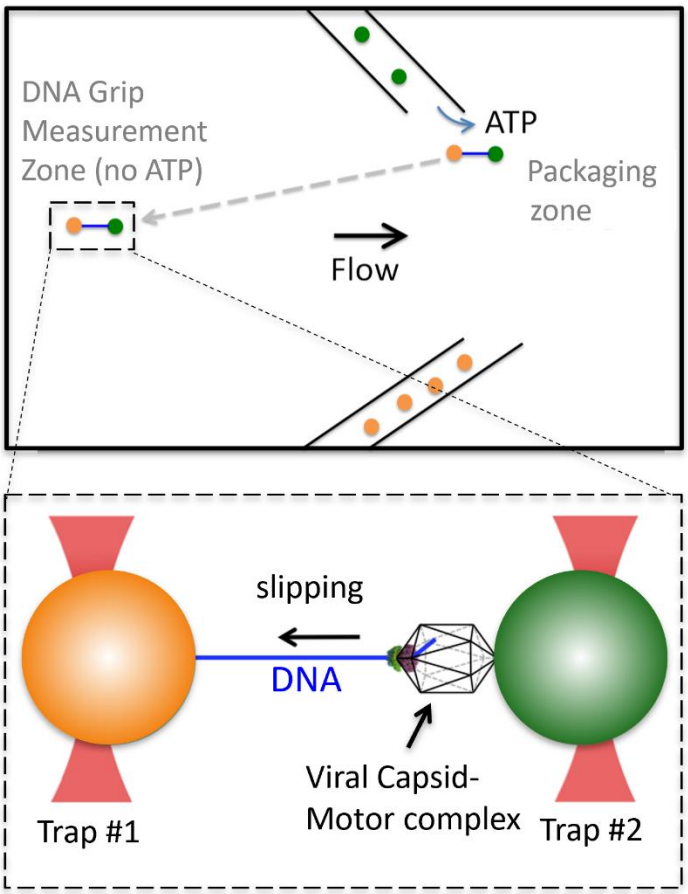

Fig. 1 Schematic illustration of the experiment. Lambda packaging complexes stalled with γ-S-ATP are attached by the unpackaged DNA end to a microsphere (orange) and dispensed by a micro-capillary tube into a fluid chamber and trapped with optical tweezers. This microsphere is then brought near a second trapped microsphere coated with antibodies that bind the capsid (green). A second capillary tube dispenses a solution containing ATP and the motor begins to package the DNA. After ~1.5-6 kbp of DNA (blue) is packaged, the complex is rapidly moved away from the tube dispensing ATP (see dashed arrow) and into a region of the chamber (the "grip measurement zone") containing either no nucleotides, γ-S-ATP, AMP-PNP, or ADP. A small stretching force (5 pN) is applied so that the length of the DNA outside the capsid versus time can be measured.

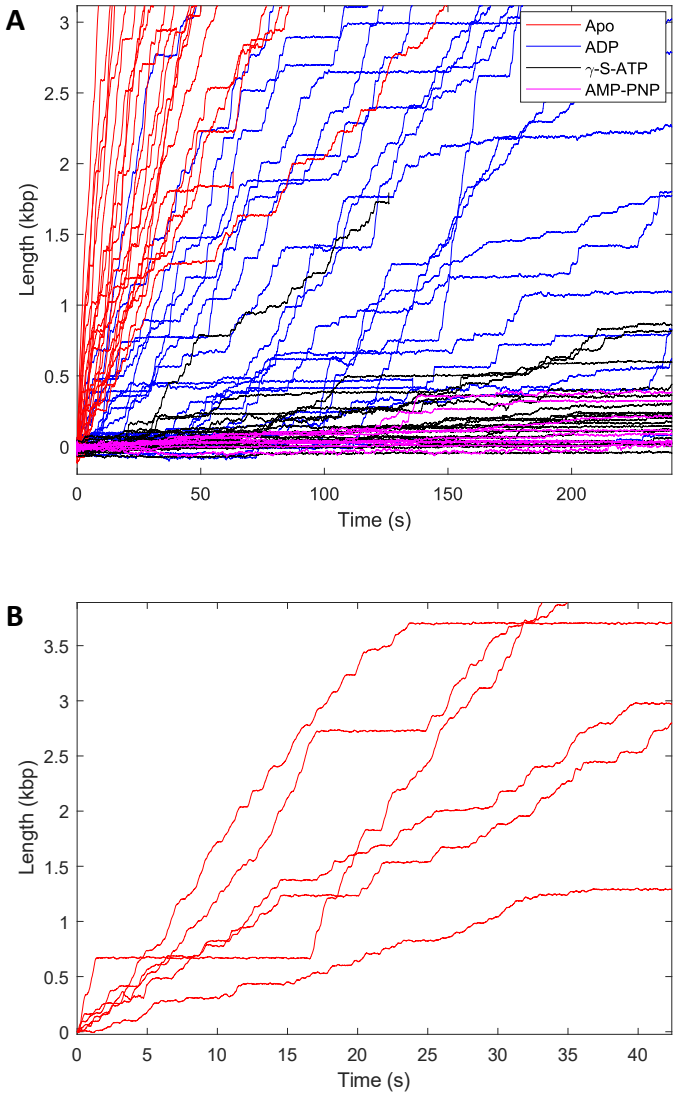

Fig. 2 (A) Representative measurements of length of DNA that has slipped out of the capsid vs. time, showing pauses (motor gripping events). Each line is a measurement on a single complex in a solution with either no nucleotides ("apo" state, red lines), ADP (0.5 mM, blue), γ-S-ATP (0.5 mM, black), or AMP-PNP (0.5 mM, magenta). **(B)** Zoomed in plot showing examples of measurements in the no nucleotide condition, where the pauses can clearly be seen.

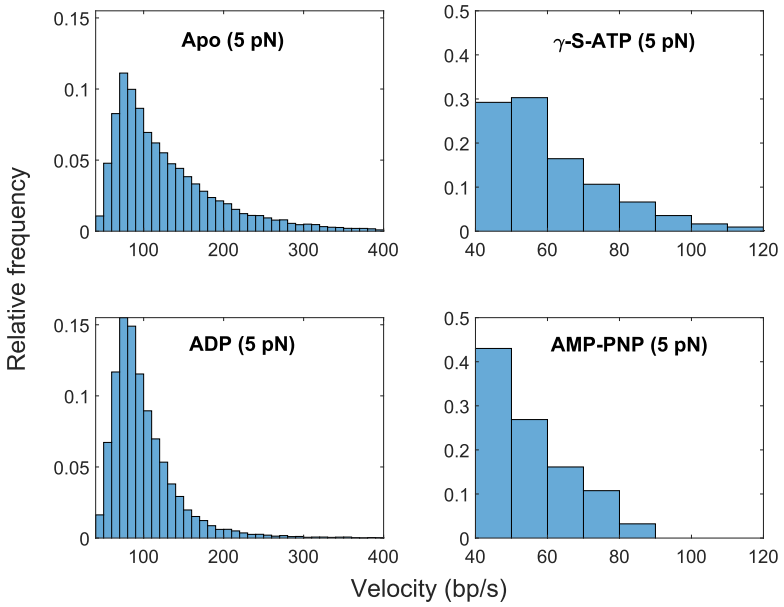

Fig 3. Distributions of transient slipping velocities measured in 1 s time intervals in each of the indicated conditions. Note that a different x-axis scale is used for the γ-S-ATP and AMP-PNP histograms because of the generally slower slipping velocities exhibited for these. For these calculations, and those in the subsequent figures, periods of slipping vs. gripping were determined using the 3σ velocity threshold criteria (see methods). Note that these distributions include only the velocities measured during slipping, whereas those plotted for T4 in Ref. 31 include the pauses (gripping events) and therefore have an additional peak around zero velocity.

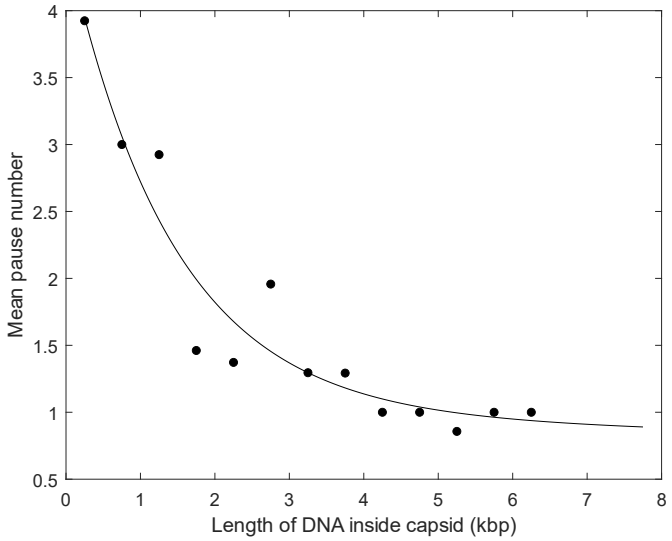

Fig 4. Dependence of pausing frequency with no nucleotides and 5 pN force on length of DNA inside the capsid. The frequency is calculated as mean number of pauses per 500 bp length bin, averaged across all events.

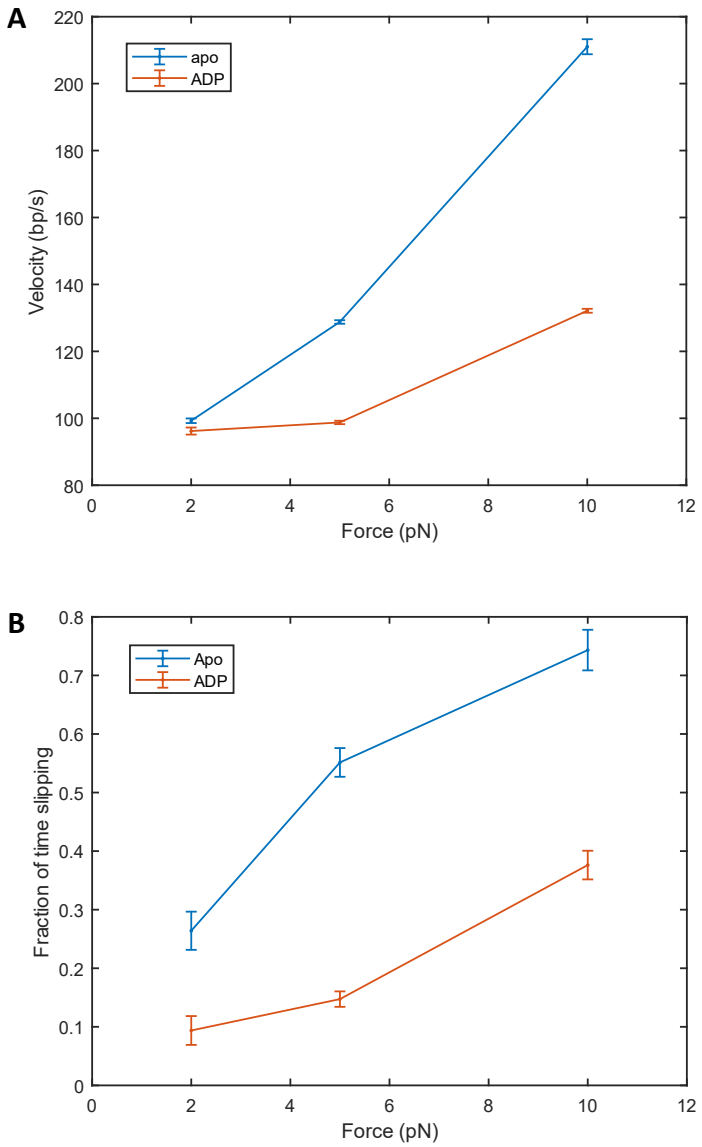

Fig. 5 (A) Dependence of the average transient slipping velocity on applied force. Error bars indicate standard errors of the means. **(B)** Dependence of the fraction of time spent slipping on applied force. This is calculated as the fraction of 1 s time bins in which slipping occurs. The blue points indicate measurements with no nucleotides and orange points indicate those with 0.5 mM ADP. Error bars indicate standard errors of the means.

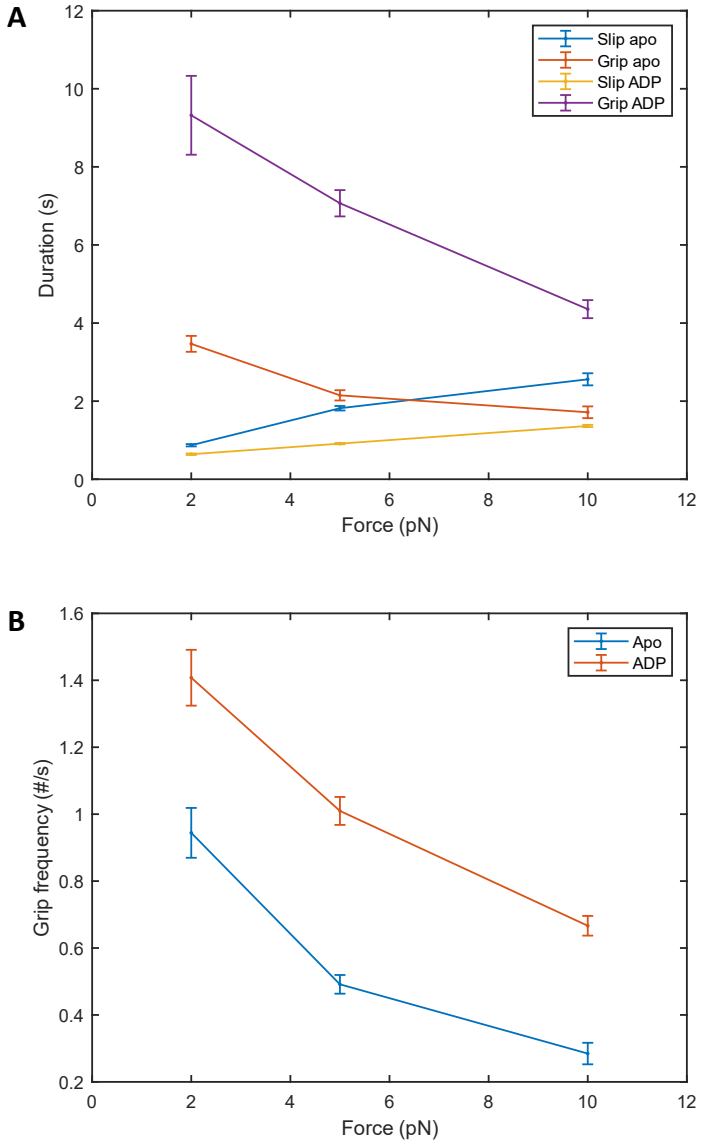

Fig. 6 (A) Dependence of the mean grip and slip durations on applied force. The blue points indicate slipping with no nucleotides, orange points gripping with no nucleotides, yellow points indicate slipping with 0.5 mM ADP, and purple points indicate gripping with 0.5 mM ADP. Error bars indicate standard errors in the means. (**B)** Dependence of the gripping frequency on applied force. Grip frequency is calculated as the number of pauses per amount of time spent slipping. The blue points indicate measurements with no nucleotides and orange points measurements with 0.5 mM ADP. Error bars indicate standard errors of the means.

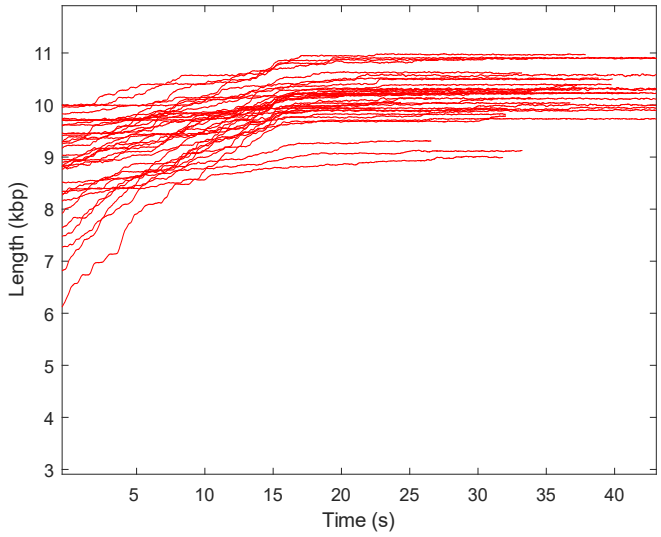

Fig. 7A Length of DNA released from the capsid vs. time measured during slipping with no nucleotides and 5 pN force. The slipping usually arrests when the length is around 10 kb, which is consistent with the full length of the DNA substrate. The ~1-2 kbp variations in the apparent ending lengths seen in this plot are attributable to measurement artifacts due to microsphere size and DNA length variations, as explained in the text.

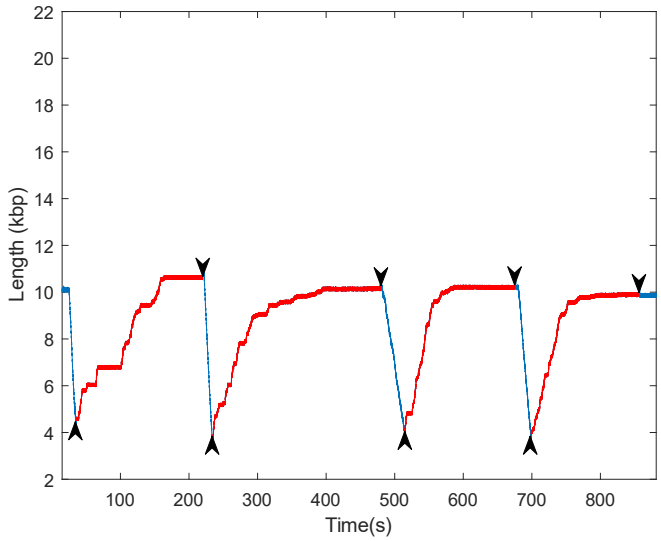

Fig. 7B Example of a repeated "package/slip/clamp/re-package" measurement with 10 pN applied force. The DNA is packaged with ATP (blue sections with decreasing length) and when the solution is changed from ATP to ADP (times indicated by upward arrows) the DNA slips out but is end clamped (red sections with increasing length). Each time the complex is moved back into ATP (indicated by downward arrows) the DNA is re-packaged again.

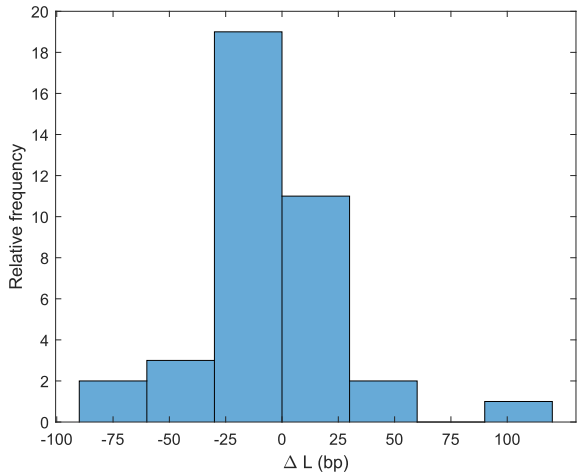

Fig. 7C Histogram of the differences in the length of DNA outside the capsid measured in repeated end clamp events with individual complexes (like the one shown in panel B).

REFERENCES

[1] Casjens, S. R. (2011). The DNA-packaging nanomotor of tailed bacteriophages. *Nature Reviews Microbiology*, *9*(9), 647-657.

[2] Rao, V. B., & Feiss, M. (2015). Mechanisms of DNA packaging by large double-stranded DNA viruses. *Annual Review of Virology*, *2*(1), 351.

[3] Hetherington, C. L., Moffitt, J. R., Jardine, P. J., & Bustamante, C. (2012). Viral DNA packaging motors. In *Comprehensive Biophysics* (pp. 420-446). Elsevier Inc.

[4] Catalano, C. E., & Morais, M. C. (2021). Viral genome packaging machines: Structure and enzymology. *The Enzymes*, *50*, 369-413.

[5] Riemer, S. C., & Bloomfield, V. A. (1978). Packaging of DNA in bacteriophage heads: some considerations on energetics. *Biopolymers*, *17*(3), 785-794.

[6] Kindt, J., Tzlil, S., Ben-Shaul, A., & Gelbart, W. M. (2001). DNA packaging and ejection forces in bacteriophage. *Proceedings of the National Academy of Sciences*, *98*(24), 13671-13674.

[7] Purohit, P. K., Kondev, J., & Phillips, R. (2003). Mechanics of DNA packaging in viruses. *Proceedings of the National Academy of Sciences*, *100*(6), 3173-3178.

[8] Ali, I., Marenduzzo, D., & Yeomans, J. M. (2006). Polymer packaging and ejection in viral capsids: shape matters. *Physical Review Letters*, *96*(20), 208102.

[9] Forrey, C., & Muthukumar, M. (2006). Langevin dynamics simulations of genome packing in bacteriophage. *Biophysical Journal*, *91*(1), 25-41.

[10] Petrov, A. S., & Harvey, S. C. (2008). Packaging double-helical DNA into viral capsids: structures, forces, and energetics. *Biophysical journal*, *95*(2), 497-502.

[11] Lyubimov, A. Y., Strycharska, M., & Berger, J. M. (2011). The nuts and bolts of ring-translocase structure and mechanism. *Current Opinion in Structural Biology*, *21*(2), 240-248.

[12] Allemand, J. F., Maier, B., & Smith, D. E. (2012). Molecular motors for DNA translocation in prokaryotes. *Current Opinion in Biotechnology*, *23*(4), 503-509.

[13] Liu, S., Chistol, G., & Bustamante, C. (2014). Mechanical operation and intersubunit coordination of ring-shaped molecular motors: insights from single-molecule studies. *Biophysical Journal*, *106*(9), 1844-1858.

[14] Smith, D. E., Tans, S. J., Smith, S. B., Grimes, S., Anderson, D. L., & Bustamante, C. (2001). The bacteriophage φ29 portal motor can package DNA against a large internal force. *Nature*, *413*(6857), 748-752.

[15] Rickgauer, J. P., Fuller, D. N., Grimes, S., Jardine, P. J., Anderson, D. L., & Smith, D. E. (2008). Portal motor velocity and internal force resisting viral DNA packaging in bacteriophage ϕ29. *Biophysical Journal*, *94*(1), 159-167.

[16] Fuller, D. N., Raymer, D. M., Kottadiel, V. I., Rao, V. B., & Smith, D. E. (2007). Single phage T4 DNA packaging motors exhibit large force generation, high velocity, and dynamic variability. *Proceedings of the National Academy of Sciences*, *104*(43), 16868-16873.

[17] Fuller, D. N., Raymer, D. M., Rickgauer, J. P., Robertson, R. M., Catalano, C. E., Anderson, D. L., ... & Smith, D. E. (2007). Measurements of single DNA molecule packaging dynamics in bacteriophage λ reveal high forces, high motor processivity, and capsid transformations. *Journal of Molecular Biology*, *373*(5), 1113-1122.

[18] Keller, N., delToro, D. J., & Smith, D. E. (2018). Single-molecule measurements of motor-driven viral DNA packaging in bacteriophages Phi29, lambda, and T4 with optical tweezers. In *Molecular Motors* (pp. 393-422). Humana Press, New York, NY.

[19] Liu, S., Tafoya, S., & Bustamante, C. (2017). Deciphering the Molecular Mechanism of the Bacteriophage φ29 DNA Packaging Motor. In *Optical Tweezers* (pp. 343-355). Humana Press, New York, NY.

[20] Chemla YR, Aathavan K, Michaelis J, Grimes S, Jardine PJ, Anderson DL, Bustamante C. Mechanism of force generation of a viral DNA packaging motor. *Cell.* 2005 Sep 9;122(5):683-92.

[21] Aathavan K, Politzer AT, Kaplan A, Moffitt JR, Chemla YR, Grimes S, Jardine PJ, Anderson DL, Bustamante C. Substrate interactions and promiscuity in a viral DNA packaging motor. *Nature*. 2009 Oct;461(7264):669-73.

[22] Tsay, J. M., Sippy, J., Feiss, M., & Smith, D. E. (2009). The Q motif of a viral packaging motor governs its force generation and communicates ATP recognition to DNA interaction. *Proceedings of the National Academy of Sciences*, *106*(34), 14355-14360.

[23] Tsay JM, Sippy J, Andrews BT, Draper B, Rao V, Catalano CE, Feiss M, Smith DE. Mutations altering a structurally conserved loop-helix-loop region of a viral packaging motor change DNA translocation velocity and processivity. *Journal of Biological Chemistry*. 2010 Jul 30;285(31):24282-9.

[24] delToro D, Ortiz D, Ordyan M, Sippy J, Oh CS, Keller N, Feiss M, Catalano CE, Smith DE. Walker-A motif acts to coordinate ATP hydrolysis with motor output in viral DNA packaging. *Journal of Molecular Biology.* 2016 Jul 3;428(13):2709-29.

[25] Ortiz D, delToro D, Ordyan M, Pajak J, Sippy J, Catala A, Oh CS, Vu A, Arya G, Feiss M, Smith DE. Evidence that a catalytic glutamate and an 'Arginine Toggle' act in concert to mediate ATP hydrolysis and mechanochemical coupling in a viral DNA packaging motor. *Nucleic Acids Research.* 2019 Feb 20;47(3):1404-15.

[26] delToro D, Ortiz D, Ordyan M, Pajak J, Sippy J, Catala A, Oh CS, Vu A, Arya G, Smith DE, Catalano CE, Feiss M. Functional dissection of a viral DNA packaging Machine's Walker B Motif. *Journal of Molecular Biology*. 2019 Nov 8;431(22):4455-74.

[27] Moffitt, J. R., Chemla, Y. R., Aathavan, K., Grimes, S., Jardine, P. J., Anderson, D. L., & Bustamante, C. (2009). Intersubunit coordination in a homomeric ring ATPase. *Nature*, *457*(7228), 446-450.

[28] Chistol G, Liu S, Hetherington CL, Moffitt JR, Grimes S, Jardine PJ, Bustamante C. High degree of coordination and division of labor among subunits in a homomeric ring ATPase. *Cell.* 2012 Nov 21;151(5):1017-28.

[29] Liu S, Chistol G, Hetherington CL, Tafoya S, Aathavan K, Schnitzbauer J, Grimes S, Jardine PJ, Bustamante C. A viral packaging motor varies its DNA rotation and step size to preserve subunit coordination as the capsid fills. *Cell.* 2014 Apr 24;157(3):702-13.

[30] Berndsen, Z. T., Keller, N., & Smith, D. E. (2015). Continuous allosteric regulation of a viral packaging motor by a sensor that detects the density and conformation of packaged DNA. *Biophysical Journal*, *108*(2), 315-324.

[31] Ordyan, M., Alam, I., Mahalingam, M., Rao, V. B., & Smith, D. E. (2018). Nucleotide-dependent DNA gripping and an end-clamp mechanism regulate the bacteriophage T4 viral packaging motor. *Nature Communications*, *9*(1), 1-9.

[32] Sun S, Kondabagil K, Draper B, Alam TI, Bowman VD, Zhang Z, Hegde S, Fokine A, Rossmann MG, Rao VB. The structure of the phage T4 DNA packaging motor suggests a mechanism dependent on electrostatic forces. *Cell*. 2008 Dec 26;135(7):1251-62.

[33] Hilbert BJ, Hayes JA, Stone NP, Duffy CM, Sankaran B, Kelch BA. Structure and mechanism of the ATPase that powers viral genome packaging. *Proceedings of the National Academy of Sciences.* 2015 Jul 21;112(29):E3792-9.

[34] Mao H, Saha M, Reyes-Aldrete E, Sherman MB, Woodson M, Atz R, Grimes S, Jardine PJ, Morais MC. Structural and molecular basis for coordination in a viral DNA packaging motor. *Cell Reports*. 2016 Mar 1;14(8):2017-29.

[35] Woodson M, Pajak J, Mahler BP, Zhao W, Zhang W, Arya G, White MA, Jardine PJ, Morais MC. A viral genome packaging motor transitions between cyclic and helical symmetry to translocate dsDNA. *Science Advances*. 2021 May 7;7(19):eabc1955.

[36] Castillo JP, B Tong A, Tafoya S, Jardine PJ, Bustamante C. A DNA packaging motor inchworms along one strand allowing it to adapt to alternative double-helical structures. *Nature communications.* 2021 Jun 8;12(1):1-8.

[37] Pajak J, Dill E, Reyes-Aldrete E, White MA, Kelch BA, Jardine PJ, Arya G, Morais MC. Atomistic basis of force generation, translocation, and coordination in a viral genome packaging motor. *Nucleic Acids Research.* 2021 Jun 21;49(11):6474-88.

[38] Feiss, M., & Catalano, C. E. (2005). Bacteriophage lambda terminase and the mechanism of viral DNA packaging. In *Viral Genome Packaging Machines: Genetics, Structure, and Mechanism* (pp. 5-39). Springer, Boston, MA.

[39] Rao, Venigalla B., and Michael Feiss. "The Bacteriophage DNA Packaging Motor." *Annual Review of Genetics* 42 (2008): 647-681.

[40] Yang Q, Catalano CE, Maluf NK. Kinetic analysis of the genome packaging reaction in bacteriophage λ. *Biochemistry*. 2009 Nov 17;48(45):10705-15.

[41] Andrews, B. T., & Catalano, C. E. (2012). The enzymology of a viral genome packaging motor is influenced by the assembly state of the motor subunits. *Biochemistry*, *51*(46), 9342-9353.

[42] Andrews, B. T., & Catalano, C. E. (2013). Strong subunit coordination drives a powerful viral DNA packaging motor. *Proceedings of the National Academy of Sciences*, *110*(15), 5909-5914.

[43] Yang, Q., Maluf, N. K., & Catalano, C. E. (2008). Packaging of a unit-length viral genome: the role of nucleotides and the gpD decoration protein in stable nucleocapsid assembly in bacteriophage λ. *Journal of Molecular Biology*, *383*(5), 1037-1048.

[44] Tomka, M. A., & Catalano, C. E. (1993). Kinetic characterization of the ATPase activity of the DNA packaging enzyme from bacteriophage. lambda. *Biochemistry*, *32*(45), 11992-11997.

[45] Woods, L., & Catalano, C. E. (1999). Kinetic characterization of the GTPase activity of phage λ terminase: Evidence for communication between the two “NTPase” catalytic sites of the enzyme. *Biochemistry*, *38*(44), 14624-14630.

[46] Keller, N. A. (2016). *Single Molecule Dynamics of Viral DNA Packaging Using Optical Tweezers*. PhD Thesis, University of California, San Diego.

[47] Marenduzzo, D., Orlandini, E., Stasiak, A., Sumners, D. W., Tubiana, L., & Micheletti, C. (2009). DNA–DNA interactions in bacteriophage capsids are responsible for the observed DNA knotting. *Proceedings of the National Academy of Sciences*, *106*(52), 22269-22274.

[48] Keller, N., Grimes, S., Jardine, P. J., & Smith, D. E. (2016). Single DNA molecule jamming and history-dependent dynamics during motor-driven viral packaging. *Nature Physics*, *12*(8), 757-761.

[49] Raymer, D. M., & Smith, D. E. (2007). Spontaneous knotting of an agitated string. *Proceedings of the National Academy of Sciences*, *104*(42), 16432-16437.

[50] Plesa C, Verschueren D, Pud S, Van Der Torre J, Ruitenberg JW, Witteveen MJ, Jonsson MP, Grosberg AY, Rabin Y, Dekker C. Direct observation of DNA knots using a solid-state nanopore. *Nature Nanotechnology.* 2016 Dec;11(12):1093-7.

[51] Evilevitch, A., Lavelle, L., Knobler, C. M., Raspaud, E., & Gelbart, W. M. (2003). Osmotic pressure inhibition of DNA ejection from phage. *Proceedings of the National Academy of Sciences*, *100*(16), 9292-9295.

[52] Ward A, Hilitski F, Schwenger W, Welch D, Lau AW, Vitelli V, Mahadevan L, Dogic Z. Solid friction between soft filaments. *Nature Materials*. 2015 Jun;14(6):583-8.

[53] Grayson, P., Han, L., Winther, T., & Phillips, R. (2007). Real-time observations of single bacteriophage λ DNA ejections in vitro. *Proceedings of the National Academy of Sciences*, *104*(37), 14652-14657.

[54] Sternberg, N., & Coulby, J. (1987). Recognition and cleavage of the bacteriophage P1 packaging site (pac): I. Differential processing of the cleaved ends in vivo. *Journal of Molecular Biology*, *194*(3), 453-468.

[55] delToro, D., & Smith, D. E. (2014). Accurate measurement of force and displacement with optical tweezers using DNA molecules as metrology standards. *Applied Physics Letters*, *104*(14), 143701.